



Remote Sensing of Climate-Vegetation Dynamics and Their Effects on Ecosystems

Chung-Te Chang^{1,2,*} , Jyh-Min Chiang^{1,2} and Junhu Dai^{3,4}

¹ Taiwan International Graduate Program (TIGP)—Ph.D. Program on Biodiversity, Tunghai University, Taichung 407224, Taiwan; jyhmin@thu.edu.tw

² Center for Ecology and Environment, Tunghai University, Taichung 407224, Taiwan

³ Key Laboratory of Land Surface Pattern and Simulation, Institute of Geographic Sciences and Natural Resources Research, China Phenological Observation Network, Chinese Academy of Sciences, Beijing 100101, China; daijh@igsnr.ac.cn

⁴ University of Chinese Academy of Sciences, Beijing 100049, China

* Correspondence: chungtechang@thu.edu.tw; Tel.: +886-4-2359-0121

Vegetation phenology, i.e., the recurring events of plant growth, is an integrated indicator delineating terrestrial ecosystem dynamics [1,2] and plays a key role in realizing climate-phenology-hydrology associations in response to climate change, natural disturbances, and anthropogenic forces [3–5]. A comprehension of the intertwined, concurrent relationship between vegetation growth and climatic variations is critical to understanding the major regulation of biotic and abiotic factors in ecosystem dynamics. Several decades of in situ plant phenological records from the IPG (International Phenological Garden—<http://ipg.hu-berlin.de/>, accessed on 1 May 2023), NPN (National Phenology Network—<https://www.usanpn.org/>, accessed on 1 May 2023), and CPON (Chinese Phenological Observation Network—<http://www.cpon.ac.cn/>, accessed on 1 May 2023) have revealed that earlier leaf unfolding and later senescence have resulted in a longer growing season in many regions [6–9]. Temperature is the main controlling factor in plant phenological dynamics in the temperate region [6,7,9–11]. However, recent reports show that the importance of later senescence on the extension of the growing season is greater than the contribution of earlier green-up [8,12]. Information from ground observation is valuable, but its geographic extent is limited (Figure 1), and long-term observations are rare in harsh settings such as arctic, tundra, desert, and tropics/subtropics [13,14].

With the advances in remote sensing techniques over the past decades, vegetation indices (VIs), such as the normalized difference vegetation index (NDVI) and the enhanced vegetation index (EVI), have been utilized widely to detect land surface phenology (LSP), from the landscape to global scales (Figure 1; [15–17]). The patterns in VI-derived phenological metrics, including the SOS (start of the growing season), the EOS (end of the growing season), and the LOS (length of the growing season), have been extensively investigated. These local patterns are closely linked to three dominant drivers of phenology: temperature, water, and light [17–21]. Additionally, they are influenced by large-scale atmospheric fluctuations, such as ENSO (El Niño–Southern Oscillation) [17,22–25]. Many researchers have pointed out that the continuing alterations in phenological patterns associated with the ongoing climatic warming require long-term attention. A study conducted at Leinhuachi Experimental Forest (LHC) in central Taiwan indicated that the shortage of spring rainfall (i.e., spring drought) related to ENSO events likely plays an important role in not only the SOS and the LOS but also the water budget (Figure 2; [5]). The LHC is projected to have more frequent and longer drought events. The increase in drought and potential land-use change can greatly affect the climate-phenology-biogeochemistry relationship, which affects the provision of water resources that are important to socio-ecological systems (Figure 2). The phenological information regarding plant growth is also beneficial in identifying tree species and their composition in forested landscapes [26]. The application of a near-surface



Citation: Chang, C.-T.; Chiang, J.-M.; Dai, J. Remote Sensing of Climate-Vegetation Dynamics and Their Effects on Ecosystems. *Remote Sens.* **2023**, *15*, 5097. <https://doi.org/10.3390/rs15215097>

Received: 9 October 2023

Revised: 20 October 2023

Accepted: 23 October 2023

Published: 25 October 2023



Copyright: © 2023 by the authors. Licensee MDPI, Basel, Switzerland. This article is an open access article distributed under the terms and conditions of the Creative Commons Attribution (CC BY) license (<https://creativecommons.org/licenses/by/4.0/>).

remote sensing approach based on a digital camera (i.e., the PhenoCam) (Figure 1) over the last decade is helpful for collecting time-series data concerning plant development across various climates and biomes. The PhenoCam also provides ground-truth or validation for remotely sensed data [27–30] and carbon (C) flux calculations [31]. The real-time images can capture the effects of sporadic events on vegetation on the landscape scale [32]; this has often been a challenge for satellite images due to the frequent cloud cover in the upper atmosphere.

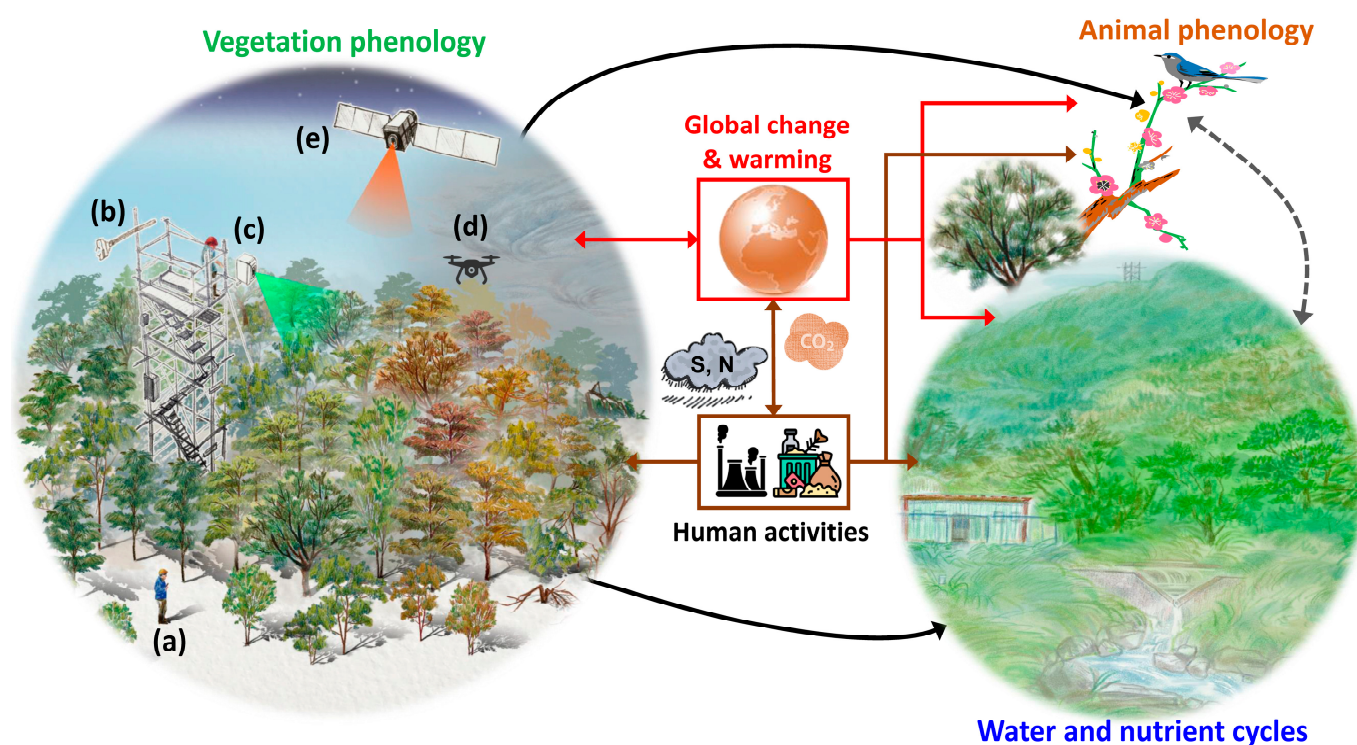


Figure 1. The effects of climate warming and anthropogenic activities on vegetation phenology and animal phenology, and the subsequent impacts on the ecosystem structure and function. The approaches used to monitor vegetation phenology include (a) in situ observation, (b) CO₂ flux instrumentation, (c) a near-surface digital camera (PhenoCam), (d) an unmanned aerial vehicle (UAV) or drone, and (e) satellite images. The black and red arrows stand for the possible impacts of human activities and climatic warming on vegetation phenology and ecosystem function, and blue arrows indicate the associations between vegetation phenology and animal phenology and hydrological and biogeochemical cycling.

In addition to climatic and anthropogenic factors, nutrients and their interactions with water availability can also affect vegetation growth and phenology in regions limited by nutrients [33,34]. Concerns have been raised around a nutritional phenological mismatch between consumers (foraging species) and resources (habitats) owing to rapid climate change, which will likely alter the above- and below-ground vegetation biomass (productivity) and animal reproduction [35,36]. Further exploration is needed not only into the phenological modeling of individual phenological indicators from the plant to the landscape scale, but also into the interactions between the climate and phenology, phenology and hydrology, phenology and biogeochemistry, animal and vegetation phenology, and new emerging fields (Figures 1 and 2). This Special Issue aims to encompass the latest developments in LSP responses to hydroclimate regimes, the application of phenological information to identify tree species or the species composition of forest ecosystems, and the subsequent effects on ecosystems.

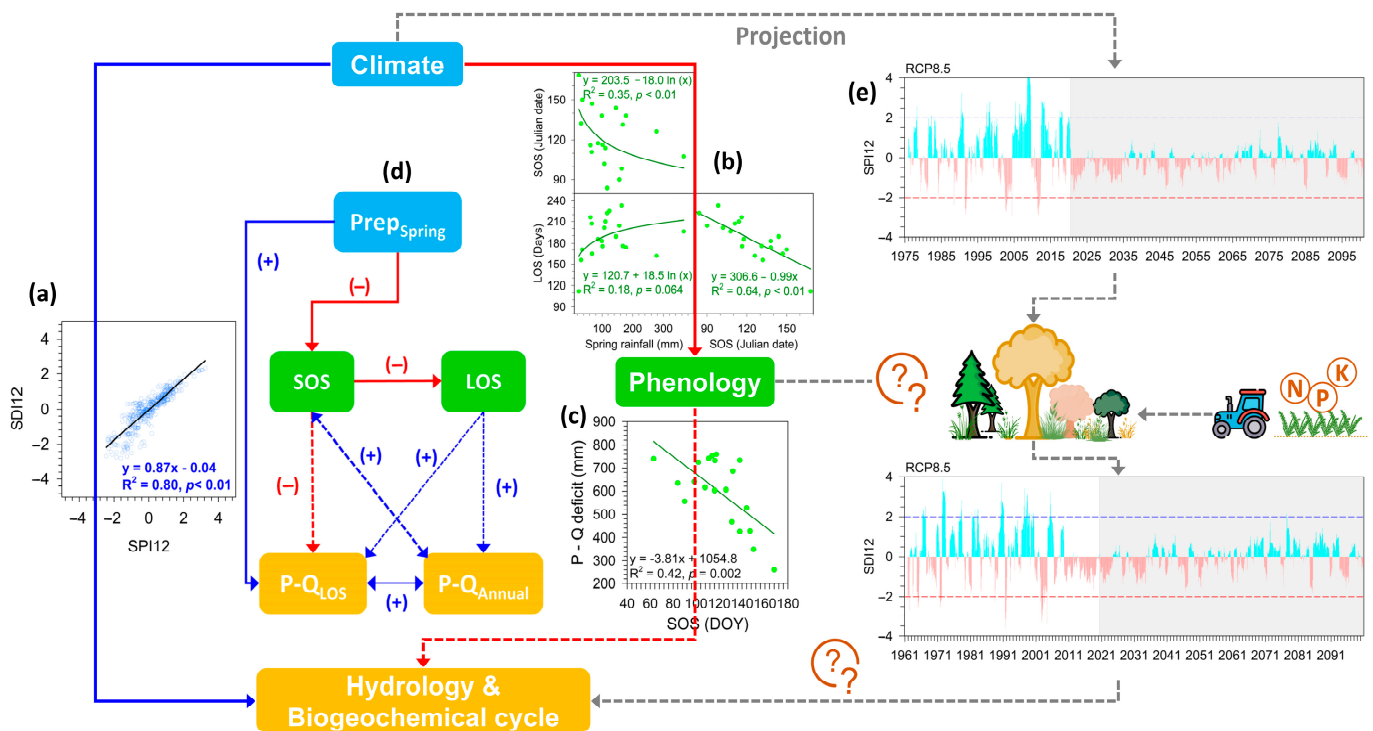


Figure 2. The interrelationships among the climate, vegetation growth, and hydrology of watershed #4 at the Leinhuachi Experimental Forest (LHC), central Taiwan [5]. (a) The relationship between meteorological drought and hydrological drought; (b) the relationship between seasonal rainfall and phenology; (c) the relationship between phenology and water budget (e.g., P-Q deficit [precipitation minus streamflow]); (d) the concept of interrelationships among the climate, phenology, and hydrology based on an SEM (structural equation model); and (e) the projected meteorological and hydrological droughts under a high-emission scenario (RCP8.5) and land-use alterations, and their potential impacts on vegetation growth, the water budget, and the biogeochemical cycle. SPI12 and SDI12 stand for Standardized Precipitation Index and Streamflow Drought Index at 12-month time scales, respectively; these are commonly utilized to characterize meteorological and hydrological drought conditions. Blue lines indicate positive effects, while red lines indicate negative effects. The gray dashed lines stand for uncertain associations among observations.

In this Special Issue, we share current studies and development of vegetation-climate relationships, land surface phenology based on satellite images, PhenoCam observations, and the possible effects on the hydrology and biogeochemical cycles of ecosystems. After calling for studies during 2022–2023, we published 10 papers in this Special Issue, with the study regions covering Asia, Europe, Russia, and North America. The topics include the associations between vegetation and the hydroclimate, the applications of LSP across landscapes, and the applications of the PhenoCam.

To investigate vegetation and hydroclimate associations, Yang et al. [37] used GIMMS NDVI3g (third-generation GIMMS [Global Inventory Modeling and Mapping Studies] NDVI from AVHRR sensors) to explore elevational gradients and vegetation types responding to the climate in arid central Asia (ACA) from 1982 to 2015. The results indicate that the eastern ACA is greening (>300 m) as a result of increased growing season precipitation; in contrast, the western ACA is browning (<300 m) due to decreasing soil water and a higher temperature combined with little precipitation. Medvedkov et al. [38] assessed the influences of various degrees of permafrost on boreal vegetation growth on thermal conditions at the northern Yenisei Ridge, a spruce–cedar–larch taiga landscape in Russia, and suggest that the regions covered by forest with the highest evapotranspiration had the lowest land surface temperature (LST). In contrast, higher LSTs were usually observed in areas with sparse vegetation cover characterized by a higher sensible heat and lower

evapotranspiration. Shaik et al. [39] examined the relationship between the tree canopy temperature based on a moderate imaging spectroradiometer (MODIS) LST and emissivity products with the canopy heights of various vegetation types obtained from the Global Ecosystem Dynamics Investigation (GEDI) L2A product for Sardinia, the largest Italian island. The results show that there were negative relationships between the canopy height and tree canopy temperature. More detailed synthesis is required to determine the local forest climate associated with the forest structure. Jing et al. [40] used long-term Landsat images (1988–2021) and the random forest (RF) algorithm to investigate wetland vegetation dynamics responding to the flow regime in East Dongting Lake, in the middle Yangtze River of China. They found distinct patterns in various vegetation types (*Carex* meadow, reedbed, mudflat, and shallow water) according to variations in the flow regime. For example, *Carex* meadows increased with earlier water withdrawal and a longer dry season, and reedbeds expanded independently of the increase in winter rainfall, while the lost mudflats majorly converted to meadows, reeds, and water.

For the application of phenological information, Xiao et al. [41] compared the differences in the SOS and EOS patterns derived from the GIMMS NDVI3g and MODIS NDVI datasets. They found that there were no significant trends in the SOS and the EOS during 2000 and 2015. The discrepancies were larger in the SOS than in the EOS between the two datasets, and the differences in the SOS in forests were smaller than in shrublands and grasslands in temperate China. However, the differences in the EOS in forests were higher than those in the SOS, and the discrepancies in the EOS in shrublands and grasslands were much lower than those in the SOS. The comparisons offer essential baseline information for using NDVI datasets in the study of vegetation patterns and dynamics. Polyakova et al. [42] compared two recognizing methods, random forest (RF) and generative topographic mapping (GTM), and combined the phenological variability in vegetation cover for the automated identification of tree species in coniferous–deciduous forests in western Kazan, Russia. The phenological curves of coniferous and deciduous species are separately retrieved from Sentinel-2 data, and they perform well in separating tree species to determine their composition in forest landscapes, especially using the RF approach.

To explore the applications of PhenoCam, Cui et al. [43] calculated green chromaticity coordinates (GCC) as reference data for landscape phenology across 79 deciduous broadleaf forests (DBFs) from PhenoCam Network sites in North America, and examined the feasibility for detecting LSP of commonly used NDVI, EVI, or NIRv (near-infrared reflectance of vegetation) derived from Landsat, Sentinel-2 (30 m), and MODIS products (MCD43A4, 500 m). The major findings showed that the various remotely sensed indices captured phenological metrics consistently. For the SOS, NIRv revealed a better result than EVI and NDVI; however, NDVI performed better than EVI and NIRv in deriving the EOS. On the other hand, the 30 m data indicated a prominent improvement in obtaining the SOS, while the 500 m indices outperformed the 30 m indices for detecting the EOS of DBF phenology. Vasquez et al. [44] developed a new vegetation index combining cyan (C), orange (O), and near-infrared (NIR) bands from the camera to evaluate soybean growth dynamics at Lakehead University Agriculture Research Station, Thunder Bay, Canada. They found that the $VI_{NIR,O,C}$ index showed the best relation to the leaf area index (LAI) for mid-growing seasons, while the $VI_{O,C}$ index displayed good results for the first and last stages of vegetation development. The new proposed index provides a viable means of analyzing the vegetation development of soybeans.

From field observations to large-scale monitoring, the remote sensing of climate-vegetation dynamics is critical when it comes to comprehending the complex interactions of the atmosphere, biosphere, and hydrosphere. In this Special Issue, several related topics are still touched on less frequently, and further efforts are required to extend our knowledge and synthesize it across regions, on topics such as the climate-phenology-hydrology at watersheds, the variations in LSP in biogeochemistry, and phenological projection. To evaluate future global vegetation growth and ensure the C and nitrogen (N) cycles, it is critical to consider not only climatic factors, such as the temperature, precipitation,

and cloud cover [45,46], but also the atmospheric CO₂ concentration, N deposition, or phosphorus (P) limitation [47–52], as well as land cover changes [53,54]. We also expect the collection of papers in this Special Issue to offer some inspiration for subsequent discussions and potential collaborations across regions and disciplines.

Funding: C.T. Chang, acknowledges the generous support from National Science and Technology Council, Taiwan, R.O.C. (NSTC 110-2313-B-029-002-, 111-2313-B-029-001-, 111-2321-B-029-001, 112-2321-B-029-001, and 112-2121-M-029-001).

Acknowledgments: We appreciate the Guest Editor, Academic Editor, Section Managing Editor, members of the journal office, and anonymous reviewers for their valuable suggestions for, and efforts on, earlier versions of the manuscript.

Conflicts of Interest: The authors declare no conflict of interest.

References

- Güsewell, S.; Furrer, R.; Gehrig, E.; Peitragalla, B. Changes in temperature sensitivity of spring phenology with recent climate warming in Switzerland are related to shifts of the pre-season. *Glob. Chang. Biol.* **2017**, *23*, 5189–5202. [[CrossRef](#)] [[PubMed](#)]
- Flynn, D.F.B.; Woklovich, E.M. Temperature and photoperiod drive spring phenology across all species in a temperate forest community. *New Phytol.* **2018**, *219*, 1353–1362. [[CrossRef](#)] [[PubMed](#)]
- Hwang, T.; Martin, K.L.; Vose, J.M.; Wear, D.; Miles, B.; Kim, Y.; Band, L.E. Nonstationary hydrological behavior in forested watersheds is mediated by climate-induced changes in growing season length and subsequent vegetation growth. *Water Resour. Res.* **2018**, *54*, 5359–5375. [[CrossRef](#)]
- Wang, H.; Tetzlaff, D.; Buttle, J.; Carey, S.K.; Laudon, H.; McNamara, J.P.; Spence, C.; Soulsby, C. Climate-phenology-hydrology interactions in northern high latitudes: Assessing the value of remote sensing data in catchment ecohydrological studies. *Sci. Total Environ.* **2019**, *656*, 19–28. [[CrossRef](#)] [[PubMed](#)]
- Chang, C.T.; Lee, J.Y.; Chiang, J.M.; Wang, H.C.; Huang, J.C.; Tseng, C.W.; Wang, C.H.; Fu, S.W. Characterizing the climate-phenology-hydrology associations in a subtropical forested watershed, central Taiwan. *Ecol. Indic.* **2022**, *145*, 109650. [[CrossRef](#)]
- Cayan, D.R.; Kammerdiener, S.A.; Dettinger, M.D.; Caprio, J.M.; Peterson, D.H. Changes in the onset of spring in the Western United States. *Bull. Am. Meteorol. Soc.* **2001**, *82*, 399–415. [[CrossRef](#)]
- Menzel, A.; Sparks, T.H.; Estrella, N.; Koch, E.; Aasa, A.; Ahas, R.; Alm-Kubler, K.; Bissolli, P.; Braslavská, O.; Briede, A.; et al. European phenological response to climate change matches the warming pattern. *Glob. Chang. Biol.* **2006**, *12*, 1969–1976. [[CrossRef](#)]
- Mo, F.; Zhang, J.; Wang, J.; Cheng, Z.G.; Sun, G.J.; Ren, H.X.; Zhao, X.Z.; Cheruiyot, W.K.; Kavagi, L.; Wang, J.Y.; et al. Phenological evidence from China to address rapid shifts in global flowering times with recent climate change. *Agric. For. Meteorol.* **2017**, *246*, 22–30. [[CrossRef](#)]
- Dai, J.; Wang, H.; Ge, Q. The spatial pattern of leaf phenology and its response to climate change in China. *Int. J. Biometeorol.* **2014**, *58*, 521–528. [[CrossRef](#)]
- Ge, Q.; Wang, H.; Rutishauser, T.; Dai, J. Phenological response to climate change in China: A meta-analysis. *Glob. Chang. Biol.* **2015**, *21*, 265–274. [[CrossRef](#)]
- Doi, H.; Katano, I. Phenological timings of leaf budburst with climate change in Japan. *Agric. For. Meteorol.* **2008**, *148*, 512–516. [[CrossRef](#)]
- Yang, B.; He, M.; Shishov, V.; Tychkov, I.; Vaganov, E.; Rossi, S.; Charpentier, F.; Bräuning, L.A.; Griebinger, J. New perspective on spring vegetation phenology and global climate change based on Tibetan Plateau tree-ring data. *Proc. Natl. Acad. Sci. USA* **2017**, *114*, 6966–6971. [[CrossRef](#)] [[PubMed](#)]
- Richardson, A.D.; Keenan, T.F.; Migliavacca, M.; Ryu, Y.; Sonnentag, O.; Toomey, M. Climate change, phenology, and phenological control of vegetation feedbacks to the climate system. *Agric. For. Meteorol.* **2013**, *169*, 156–173. [[CrossRef](#)]
- Chang-Yang, C.H.; Needham, J.; Lu, C.L.; Hsieh, C.F.; Sun, I.F.; McMahon, S.M. Closing the life cycle of forest trees: The difficult dynamics of seedling-to-sapling transitions in a subtropical rainforest. *J. Ecol.* **2021**, *109*, 2705–2716. [[CrossRef](#)]
- Wang, X.; Wang, T.; Liu, D.; Guo, H.; Huang, H.; Zhao, Y. Moisture-induced greening of the South Asia over the past three decades. *Glob. Chang. Biol.* **2017**, *23*, 4995–5005. [[CrossRef](#)]
- Zeng, L.; Wardlow, B.D.; Xiang, D.; Hu, S.; Li, D. A review of vegetation phenological metrics extraction using time-series, multispectral satellite data. *Remote Sens. Environ.* **2020**, *237*, 111511. [[CrossRef](#)]
- Chang, C.T.; Wang, H.C.; Huang, C. Impacts of vegetation onset time on net primary productivity in a mountainous island in Pacific Asia. *Environ. Res. Lett.* **2013**, *8*, 045030. [[CrossRef](#)]
- Chang, C.T.; Wang, S.F.; Vadeboncoeur, M.A.; Lin, T.C. Relating vegetation dynamics to temperature and precipitation at monthly and annual time scales in Taiwan using MODIS vegetation indices. *Int. J. Remote Sens.* **2014**, *35*, 598–620. [[CrossRef](#)]
- Wang, H.; Dai, J.; Zheng, J.; Ge, Q. Temperature sensitivity of plant phenology in temperate and subtropical regions of China from 1850 to 2009. *Int. J. Climatol.* **2015**, *35*, 913–922. [[CrossRef](#)]

20. Deng, H.; Yin, Y.; Wu, S.; Xu, X. Contrasting drought impacts on the start of phenological growing season in northern China during 1982–2015. *Int. J. Climatol.* **2020**, *40*, 3330–3347. [[CrossRef](#)]
21. He, Z.; Du, J.; Chen, L.; Zhu, X.; Lin, P.; Zhao, M.; Fang, S. Impacts of recent climate extremes on spring phenology in arid-mountain ecosystems in China. *Agric. For. Meteorol.* **2018**, *260–261*, 31–40. [[CrossRef](#)]
22. Hilker, T.; Lyapustin, A.I.; Tucker, C.J.; Hall, F.G.; Myneni, R.B.; Wang, Y.; Bi, J.; de Moura, M.Y.; Sellers, P.J. Vegetation dynamics and rainfall variability of the Amazon. *Proc. Natl. Acad. Sci. USA* **2014**, *111*, 16041–16046. [[CrossRef](#)] [[PubMed](#)]
23. Suepa, T.; Qi, J.; Lawawirojwong, S.; Messina, J.P. Understanding spatio-temporal variation of vegetation phenology and rainfall seasonality in the monsoon Southeast Asia. *Environ. Res.* **2016**, *147*, 621–629. [[CrossRef](#)] [[PubMed](#)]
24. Park, K.A.; Bayarsaikhan, U.; Kim, K.R. Effects of El Niño on spring phenology of the highest mountain in north-east Asia. *Int. J. Remote Sens.* **2012**, *33*, 5268–5288. [[CrossRef](#)]
25. Mohamed, M.A.A.; Babiker, I.S.; Chen, Z.M.; Ikeda, K.; Ohta, K.; Kato, K. The role of climate variability in the inter-annual variation of terrestrial net primary production (NPP). *Sci. Total Environ.* **2004**, *332*, 123–137. [[CrossRef](#)]
26. Xu, K.; Chang, C.T.; Tian, Q.; Zeng, H.; Xie, J. Recovery of forest carbon density and carbon storage in a soil-degraded landscape in southeastern China. *Eur. J. For. Res.* **2019**, *138*, 397–413. [[CrossRef](#)]
27. Graham, E.A.; Yuen, E.M.; Robertson, G.F.; Kaiser, W.J.; Hamilton, M.P.; Rundel, P.W. Budburst and leaf area expansion measured with a novel mobile camera system and simple color thresholding. *Environ. Exp. Bot.* **2009**, *65*, 238–244. [[CrossRef](#)]
28. Richardson, A.D.; Hufkens, K.; Milliman, T.; Aubrecht, D.M.; Chen, M.; Gray, J.M.; Johnston, M.R.; Keenan, T.F.; Klosterman, S.T.; Kosmala, M.; et al. Tracking vegetation phenology across diverse North American biomes using PhenoCam imagery. *Sci. Data* **2018**, *5*, 180028. [[CrossRef](#)]
29. Klosterman, S.T.; Hufkens, K.; Gray, J.M.; Melaas, E.; Sonnentag, O.; Lavine, I.; Mitchell, L.; Norman, R.; Friedl, M.A.; Richardson, A.D. Evaluating remote sensing of deciduous forest phenology at multiple spatial scale using PhenoCam imagery. *Biogeosciences* **2014**, *11*, 4305–4320. [[CrossRef](#)]
30. Parmentier, F.J.W.; Nilsen, L.; Tømmervik, H.; Cooper, E.J. A distributed time-lapse camera network to track vegetation phenology with high temporal detail and at varying scales. *Earth Syst. Sci. Data* **2021**, *13*, 3593–3606. [[CrossRef](#)]
31. Saitoh, T.M.; Nagai, S.; Saigusa, N.; Kobayashi, H.; Suzuki, R.; Nasahara, K.N.; Muraoka, H. Assessing the use of camera-based indices for characterizing canopy phenology in relation to gross primary production in a deciduous broad-leaved and an evergreen coniferous forest in Japan. *Ecol. Inform.* **2012**, *11*, 45–54. [[CrossRef](#)]
32. Ide, R.; Oguma, H. Use of digital cameras for phenological observations. *Ecol. Inform.* **2010**, *5*, 339347. [[CrossRef](#)]
33. Piao, S.; Liu, Q.; Chen, A.; Janssens, I.A.; Fu, Y.; Dai, J.; Liu, L.; Lian, X.; Shen, M.; Zhu, X. Plant phenology and global climate change: Current progresses and challenges. *Glob. Chang. Biol.* **2019**, *25*, 1922–1940. [[CrossRef](#)] [[PubMed](#)]
34. Luo, Y.; El-Madany, T.; Ma, X.; Nair, R.; Jung, M.; Weber, U.; Filippa, G.; Bucher, S.F.; Moreno, G.; Cremonese, E.; et al. Nutrients and water availability constrain the seasonality of vegetation activity in a Mediterranean ecosystem. *Glob. Chang. Biol.* **2020**, *26*, 4379–4400. [[CrossRef](#)] [[PubMed](#)]
35. Choi, R.T.; Beard, K.H.; Leffler, A.J.; Kelsey, K.C.; Schmutz, J.A.; Welker, J.M. Phenological mismatch between season advancement and migration timing alters Arctic plant traits. *J. Ecol.* **2019**, *107*, 2503–2518. [[CrossRef](#)]
36. Twining, C.W.; Shipley, J.R.; Mathews, B. Climate change creates nutritional phenological mismatches. *Trends Ecol. Evol.* **2022**, *37*, 736–739. [[CrossRef](#)]
37. Yang, Y.; Huang, W.; Xie, T.; Li, C.; Deng, Y.; Chen, J.; Liu, Y.; Ma, S. Elevation gradients limit the antiphase trends in vegetation and its climate response in arid central Asia. *Remote Sens.* **2022**, *14*, 5922. [[CrossRef](#)]
38. Medvekov, A.; Vysotakaya, A.; Olchev, A. Detection of geocryological conditions in boreal landscapes of the southern cryolithozone using thermal infrared remote sensing data: A case study of the northern part of the Yenisei ridge. *Remote Sens.* **2023**, *15*, 291. [[CrossRef](#)]
39. Shaik, R.U.; Jallu, S.B.; Doctor, K. Unveiling temperature patterns in tree canopies across diverse heights and types. *Remote Sens.* **2023**, *15*, 2080. [[CrossRef](#)]
40. Jing, L.; Zeng, Q.; He, K.; Liu, P.; Fan, R.; Lu, W.; Lei, G.; Wen, L.; Lu, C. Vegetation dynamics in a large floodplain wetland: Flow regime is not the sole player. *Remote Sens.* **2023**, *15*, 2614. [[CrossRef](#)]
41. Xiao, J.; Huang, K.; Lin, Y.; Ren, P.; Zu, J. Assessing vegetation phenology across different biomes in temperate China—Comparing GIMMS and MODIS NDVI datasets. *Remote Sens.* **2022**, *14*, 6180. [[CrossRef](#)]
42. Polyakova, A.; Mukharamova, S.; Yermolaev, O.; Shaykhutdinova, G. Automated recognition of tree species composition of forest communities using Sentinel-2 satellite data. *Remote Sens.* **2023**, *15*, 329. [[CrossRef](#)]
43. Cui, K.; Yang, J.; Dong, J.; Zhao, G.; Cui, Y. Comparing different spatial resolutions and indices for retrieving land surface phenology for deciduous broadleaf forests. *Remote Sens.* **2023**, *15*, 2266. [[CrossRef](#)]
44. Vasquez, R.A.R.; Heenkenda, M.K.; Nelson, R.; Serrano, L.S. Developing a new vegetation index using cyan, orange, and near infrared bands to analyze soybean growth dynamics. *Remote Sens.* **2023**, *15*, 2888. [[CrossRef](#)]
45. Liu, Y.; Wu, C.; Wang, X.; Jassal, R.S.; Gonsamo, A. Impacts of global change on peak vegetation growth and its timing in terrestrial ecosystems of the continental US. *Glob. Planet. Chang.* **2021**, *207*, 103657. [[CrossRef](#)]
46. Gonsamo, A.; Chen, J.M.; Ooi, Y.W. Peak season plant activity shift towards spring is reflected by increasing carbon uptake by extratropical ecosystems. *Glob. Chang. Biol.* **2017**, *24*, 2117–2128. [[CrossRef](#)]

47. LeBauer, D.S.; Treseder, K.K. Nitrogen limitation of net primary productivity in terrestrial ecosystems is globally distributed. *Ecology* **2008**, *89*, 371–379. [[CrossRef](#)]
48. Pan, Y.; Birdsey, R.; Hom, J.; McCullough, K. Separating effects of changes in atmospheric deposition, climate, and land-use on carbon sequestration of U.S. mid-Atlantic temperate forests. *For. Ecol. Manag.* **2009**, *259*, 151–164. [[CrossRef](#)]
49. Schulte-Uebbing, L.; de Vries, W. Global-scale impacts of nitrogen deposition on tree carbon sequestration in tropical, temperate, and boreal forests: A meta-analysis. *Glob. Chang. Biol.* **2017**, *24*, e416–e431. [[CrossRef](#)]
50. Guo, M.; Wu, C.; Peng, J.; Lu, L.; Li, S. Identifying contributions of climatic and atmospheric changes to autumn phenology over mid-high latitudes of Northern Hemisphere. *Glob. Planet. Chang.* **2021**, *197*, 103396. [[CrossRef](#)]
51. Wang, X.; Wu, C.; Zhang, X.; Li, Z.; Liu, Z.; Gonsamo, A.; Ge, Q. Satellite-observed decrease in the sensitivity of spring phenology to climate change under high nitrogen deposition. *Environ. Res. Lett.* **2020**, *15*, 094055. [[CrossRef](#)]
52. Terrer, C.; Jackson, R.B.; Prentice, I.C.; Keenan, T.F.; Kaiser, C.; Vicca, S.; Fisher, J.B.; Reich, P.B.; Stocker, B.D.; Hungate, B.A.; et al. Nitrogen and phosphorus constrain the CO₂ fertilization of global plant biomass. *Nat. Clim. Chang.* **2019**, *9*, 684–689. [[CrossRef](#)]
53. Peñuelas, J.; Ciais, P.; Canadell, J.G.; Janssens, I.A.; Fernández-Martínez, M.; Carnier, J.; Obersteiner, M.; Piao, S.; Vautard, R.; Sardans, J. Shifting from a fertilization-dominated to a warming-dominated period. *Nat. Ecol. Evol.* **2017**, *1*, 1438–1445. [[CrossRef](#)] [[PubMed](#)]
54. Huang, K.; Xia, J.; Wang, Y.; Ahlström, A.; Chen, J.; Cook, R.B.; Cui, E.; Fang, Y.; Fisher, J.B.; Huntzinger, D.N.; et al. Enhanced peak growth of global vegetation and its key mechanisms. *Nat. Ecol. Evol.* **2018**, *2*, 1897–1905. [[CrossRef](#)] [[PubMed](#)]

Disclaimer/Publisher’s Note: The statements, opinions and data contained in all publications are solely those of the individual author(s) and contributor(s) and not of MDPI and/or the editor(s). MDPI and/or the editor(s) disclaim responsibility for any injury to people or property resulting from any ideas, methods, instructions or products referred to in the content.